Experimental investigations of Turbine Induced Damping for wave energy conversion

Rishav Raj, Rayan Anandanarayanan, Aravind George, Gautam Maurya, Prasad V. Dudhgaonkar, Abdus Samad

Abstract-**Oscillating water column (OWC) uses air turbine for the conversion of pneumatic energy to mechanical energy, is one of the simple and popular methods for wave energy extraction. The turbine induces damping (i.e. ratio of square root of the pressure drop to the volume flow rate) on the OWC which affects its overall efficiency. In the past only a few turbines have been used in order to study damping characteristics. Thus, a bi-directional airflow impulse turbine of 196 mm diameter was fabricated and tested in an oscillatory airflow test rig facility at Wave Energy and Fluids Engineering Laboratory, IIT Madras. The test rig has a piston-cylinder arrangement and the stroke length of the piston was fixed at 0.4 m. The reciprocation of the piston is achieved through the rotation of crank which was varied at a different cycle time of 6, 8, 10 and 12 s. This article reports the time series analysis of the pressure drop across the turbine and its speed. Furthermore, the turbine induced damping and its effect on turbine characteristics were estimated and studied based on the varying airflow rates.**

Keywords-**wave energy, oscillating water column, impulse turbine, test rig, turbine induced damping**

Paper ID: 1368, Track: WDD. The authors would like to thank the Ministry of Earth Sciences (project no OEC / 1516 / 128 / NIOT / ABDU), National Institute of Ocean Technology, Govt. of India for the funding to conduct this research.

R. Raj, R. Anandanarayanan, A. George, G. Maurya and A. Samad is with the Wave Energy and Fluids Engineering Lab, Department of Ocean Engineering, Indian Institute Of Technology Madras, Chennai 600036, Tamil Nadu, India. (rishavrajrnc@gmail.com , ananthnarayan1987@gmail.com, georgejr.mechengg@gmail.com , gtmaur@gmail.com, samad@iitm.ac.in)

P.V. Dudhgaonkar is with Energy and Fresh Water Group, National Institute of Ocean Technology, Chennai, India email : prasad@niot.res.in

I. INTRODUCTION

OCEAN wave is one of the renewable energy resources which has immense potential for extraction of energy [1]. Wave energy is relatively less explored as compared to the other renewable sources of energy. If compared to wind energy the wave energy has greater power intensity and is more persistent [2]. One of the popular methods for the wave energy extraction is by the method of oscillating water column (OWC) which was first conceptualized by a Japanese naval officer Yoshio Mashuda. The OWC is a hollow structure which might be oscillating or fixed and has the bottom surface exposed to the sea, in which air is trapped above the exposed sea. Due to the movement of waves, the air present in the column gets compressed and decompressed. The other end of the chamber is exposed to a turbine and in the process of alternative wave action, the air is forced to flow through the turbine which is used to harvest the energy [3]. OWCs have several advantages over other wave energy extraction devices because of its simplicity. The moving parts are not exposed to water, thus, making it reliable and easy to maintain [4].

The commonly used turbines for wave energy conversion are Wells turbine and impulse turbine. The impulse turbine shows better performance and starting characteristics when compared with Wells turbine under irregular flow conditions [5]. A one-dimensional analysis of aerodynamic characteristics of an impulse turbine was done and self-pitch-controlled guide vanes were proposed for further improving the efficiency of impulse turbine [6]. For the purpose of optimizing the hub to tip ratio (H/T) of the impulse turbine, several experiments were carried out on 0.6 and 0.7 H/T ratios of an impulse turbine with a different range of Reynold's number. It was found that the turbine performance for 0.6

 Copyright © European Tidal and Wave Energy Conference 2019

H/T was better and also gave wider Reynold's number range for higher efficiency [7].

Simulations on an OWC geometry was done by using wave data from real sea conditions and the turbine characteristics were simulated with the help of experimental data which considering quasi-steady unidirectional flow. The results showed that the turbine performance mainly depended on the turbine damping as well as input wave conditions [8]. At the Vizhinjam plant in India, an impulse turbine based wave energy plant was set up and the results showed that it worked as a better power takeoff device than the Wells turbine [9].

Capture factor defines as the ratio of the power captured by the OWC to the incident wave power. It depends on the damping which is induced by the turbine on the OWC. It also varies for different damping values and for each wave condition there is a certain damping value for which the capture factor is maximum. This damping is most affected by the wave height and time period of the wave [10], [11].

In previous analytical studies, it was noted that the damping values of 196 mm bidirectional impulse turbine (BDI) matched with the 196 mm uni-directional impulse turbine (UDI). It is seen that the UDI has higher efficiency than the BDI but BDI has better performance for a wider flow coefficient range. In an attempt to study the damping characteristics of the BDI, a 196 mm diameter turbine was manufactured, which is the scaled down model of an optimized 298 mm diameter The performance parameters of the 298 mm turbine were analytically assessed and keeping the efficiency constant the model was scaled down [12]. The experiment was carried out for a particular stroke length and different time periods. The damping characteristics were studied from the data obtained from the experiments using the non-dimensional parameters namely power coefficient, pressure coefficient and damping coefficient. The relation of turbine characteristics with the turbine induced damping was obtained. The general trend of power coefficient and pressure coefficient variation for different damping values was also found out.

II. EXPERIMENTAL SETUP AND TESTING FACILITY

The Experiments on the turbine were conducted in the Wave Energy and Fluids Engineering Lab, IIT

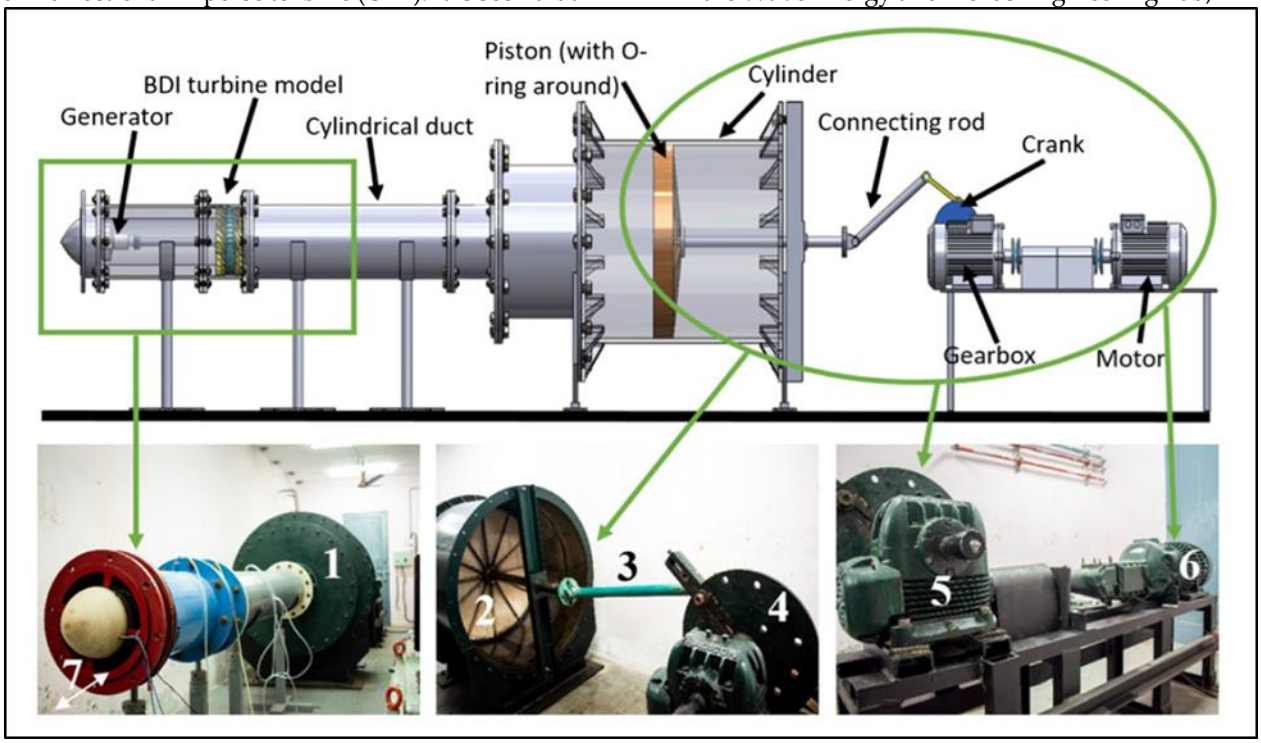

Fig. 1. Oscillating airflow test rig (1, cylinder; 2, piston; 3, connecting rod; 4, crank; 5, gearbox; 6, motor; 7, air flow passage for exhalation and inhalation [13].

Madras. The setup consists of an oscillatory air flow test rig, as shown in the Fig. 1. The rig consists of a motor, gearbox, crank, connecting rod, cylinder, piston, duct, and generator. A 3-phase induction motor (6) acts as the prime mover of the system. The motor's maximum speed is 2890 rpm, capable of delivering power up to 15 kW. It has rated voltage of 440 V and current rating of 26 A. The induction motor is driven by the variable frequency drive (VFD), which controls the input voltage and frequency, allowing the motor to run at different speeds. An automobile gearbox (5) with the gear ratio of 1:40 is used to transmit power from the crankshaft to the drive shaft. The crank (4) has a diameter of 0.5 m and is rotated by the prime mover. The connecting rod (3) has a length of 1.4 m and it connects the piston rod with the crank. It passes through a crosshead guide which enables the connecting rod to move freely outside the cylinder. A piston of diameter 1.2 m is fixed in the cylinder. The piston (2) is sealed by O-ring and lubrication is provided for minimizing friction during the reciprocating motion of the piston. The cylinder (1) has a length of 1.5 m, used to convert the mechanical energy to the electrical energy. The piston is present on one end of the cylinder and the other end has a duct in which the turbine is placed. A DC generator, 180 V, 0.745 kW is used to convert the mechanical energy of the turbine to electrical energy. A differential pressure transmitter, ABB 266DSH was used to measure the pressure drop across the turbine. The device is capable of autoconfiguration. It has a range of ±5 kPa and an accuracy of 0.06% of the calibrated range. Peppel + Fuchs universal frequency converter was used as a rotational speed frequency converter. It has a range of 0-5000rpm and an accuracy of ±5% of reading. Kimo C-310 was used as an air flow meter. It is an averaging type pitot tube multifunctional transmitter. It has a range of 0-0.9 m^3/sec with the accuracy of ±3% of the reading.

III. IMPULSE TURBINE MODEL

The tip diameter of the manufactured turbine is 196mm. It is the scaled down model of a previously manufactured 298 mm diameter turbine using the principle of dynamic similarity. The blade and the guide vane design is shown in Fig. 2. The design of 298mm diameter turbine was taken from the optimized turbine by Badhurshah and Samad [14].

TABLE. I
DESIGN SPECIFICATIONS OF THE MANUFACTURED TURBINE

Design symbols	Parameters	BDI (units in mm)
l_g	Chord length	46
l_s	Length of straight line of guide vane	23
R_a	Radius of camber of guide vane	24.5
δ	Camber angle of guide vane	60°
θ	Setting angle of guide vane	30°
S	Spacing between circular and elliptic arc	11
l	Chord length of rotor	36
E_a	Semi major axis of ellipse	82.74
R_p	Radius of circular arc on pressure side	19.86
R_i	Radius of circular arc at intersection of pressure and suction side	0.32
E_e	Semi minor axis of ellipse	27.23

The turbine blades were 3D printed using selective laser sintering (SLS).In this process, SLS uses a finely powdered polymer which is fused together with the help of lasers. Polyamide-PA2200 was used in the present case for the manufacturing of the turbine. The guide vanes (GVs) are made of stainless steel using 1.5 mm thick plates which were bent to the appropriate profile using a bending die. Grooves were made on the hub side using a 5 axis CNC machine. The GVs are fitted in the groove in

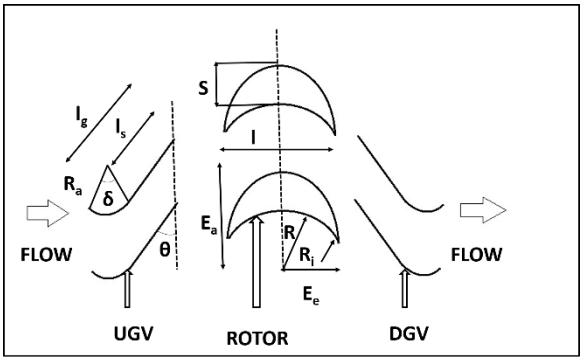

Fig.2. Design specifications of the BDI turbine

Fig.3. Fabricated guide vane

Fig.4. 3D printed rotor

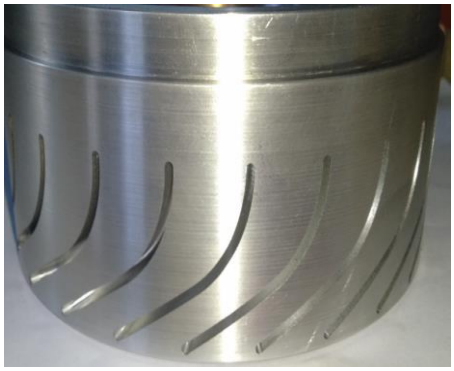

Fig. 5. Groves cut in the hub

the desired alignment. A 3 mm thick, 50 mm wide stainless steel sheet was rolled and welded to make the outer ring of the GVs.

Guide vanes (upstream guide vane (UGV), downstream guide vane (DGV)): The GVs shown in Fig. 3 are 24 in number. The whole pressure drop of this turbine takes place in the GVs. The pressure energy is converted to kinetic energy in the GVs. They also direct the flow to the turbine blades. The role of the UGV and DGV depends on the inhalation and exhalation process, which determines the direction of incoming air flow.

Rotor Blade: There are in total 38 rotor blades in the turbine. The blades use the kinetic energy of the incoming fluid to rotate the blades and hence the shaft attached to it. The manufactured rotor is shown in Fig. 4.

IV. EXPERIMENTAL PROCEDURE

The experimental testing of the 196 mm bidirectional turbine was carried out for the stroke length of 0.4 m. The stroke length was set by adjusting the connecting rod's position on the crank. The VFD was used as a controlling unit as it controls the voltage and frequency of the power supply. The frequency was changed manually in the VFD until the crank moved at the required time period (TP). The TP for the experiment was set for 6, 8, 10 and 12 seconds and testing of the turbine was done for each of those cases. When the system was switched on, the frequency was set in the VFD to obtain the desired TP of the piston oscillation. Once the motor started it made the crank to rotate. Thus, resulting in the piston movement by the help of connecting rod. The differential pressure transmitter which had its inlets fixed on the duct at the start and end of the turbine measured the pressure drop across the turbine. The pitot type flow meter was installed ahead of the turbine and it measured the flow rate in the duct.

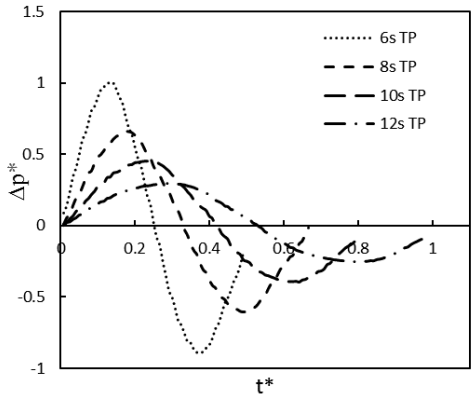

Fig. 6. Differential pressure drop for cycles of time periods

The rotational speed frequency converter was attached at the exit of the turbine shaft and measured the angular speed of the turbine.
The signals of the instruments were processed and recorded by the Lab View software installed on the computer. The sampling rate was 100 milliseconds and the data were taken for a total period of 3 minutes. Thus, a total of 5400 data samples were taken for each case. Accordingly, the values of pressure drop, flow rate and rpm were obtained.

V. RESULTS AND DISCUSSIONS

The pressure drop was measured for each time step of 0.1 sec. The graph of non-dimensional pressure drop (Δp^*) vs non-dimensional time graph (t^*) was plotted (Fig.6). Here Δp^* is $\Delta p/\Delta p_{max}$ and t^* is TP/TP_{max}. The graph was produced to show a comparison of various pressure drops for the different TPs of 6,8,10 and 12 seconds.

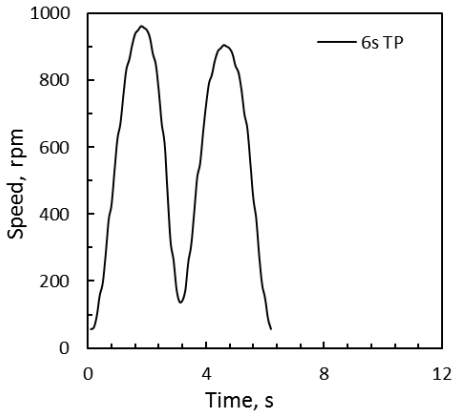

(a)

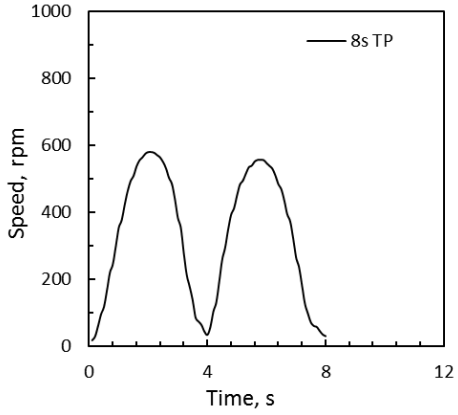

(b)

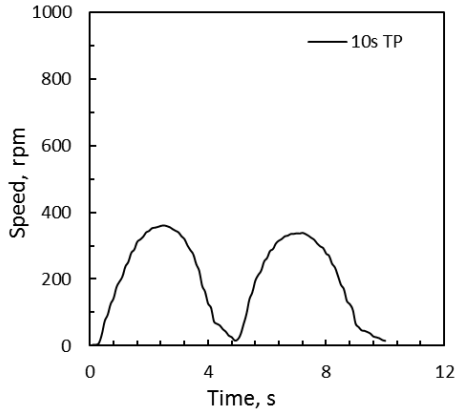

(c)

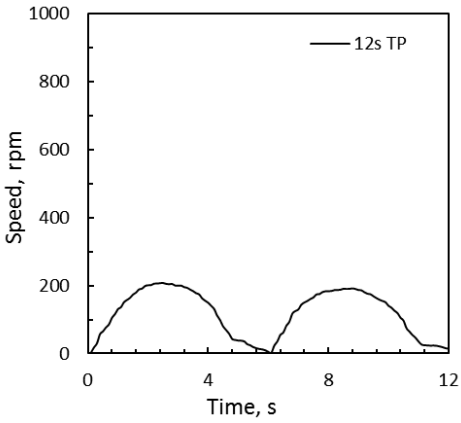

(d)

Fig. 7. Rotor speed for different time periods

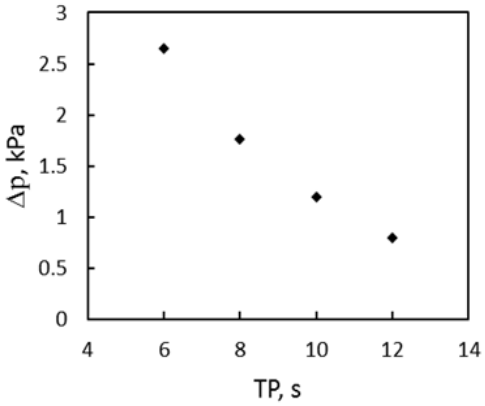

Fig. 8. Peak pressure drops obtained for different time period

All these graphs were made for the stroke length corresponding to 0.4 m. The exhalation and

inhalation of air in the turbine is depicted by the crest and the trough of the pressured drop curves. The Fig. 6 also shows the pseudo-sinusoidal variation of the pressure drop with respect to time. The reciprocating motion of the piston in the test rig causes this variation in the pressure drop. It can also be observed that the pressure drop in the inhalation process which corresponds to the trough part is less as compared to the pressure drop taking place in during the exhalation, this is because of the pressure losses due to the generator mounting at the entrance of the duct.

The Fig. 7 indicates the rotor speed variation of the impulse turbine with time. For crest and the trough parts of the pressure drop curves, the corresponding variations of the rpm is observed and it is seen that the rpm increases with the increase in the pressure drop and vice versa. The speed variations are different for the different TPs and is observed maximum in case of 6s TP and minimum in case of 12sec TP. The Fig. 8 shows the peak pressure drops obtained for each case of the TP.

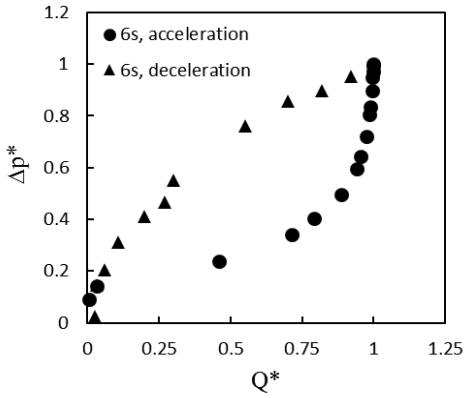

(a)

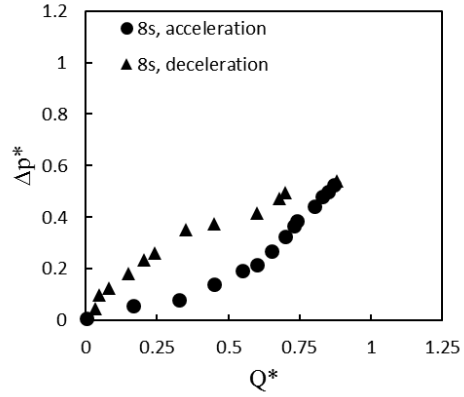

(b)

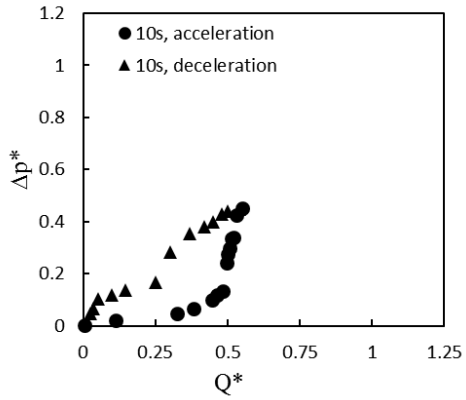

(c)

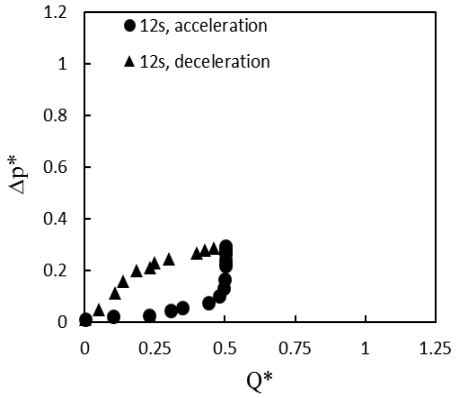

(d)

Fig. 9. Pressure drop for various flow rate values obtained during acceleration and deceleration of the half cycle

The non-dimensional pressure drop (Δp^*) vs non-dimensional flow rate (Q^*) variation is shown in Fig. 9. Here Q^* is Q/Q_{max} These represent the variation only for the exhalation part of the complete cycle because of the setup limitation of the unidirectional flowmeter. The acceleration, as well as deceleration parts of the half cycle, are represented in the figures .The variations in the acceleration and deceleration curve is because of the hysteresis effect. This phenomenon is caused due to the compressibility effect taking place within the air chamber during reciprocal movement of the piston [15]. As the magnitude of the flow rate differs for the different cycle time, the pressure drop also varies along with it. The representation of these quantities are very important as non- dimensional coefficients studied here depend on them.

The dimensional analysis of the turbine was done and three non-dimensional coefficients were studied by the help of variables such as flow rate (Q), pressure drop (Δp), angular speed (ω), turbine diameter (D), and fluid density (ρ). These coefficients are:

Turbine power coefficient: $\psi_{tw} = \frac{W_{out}\sqrt{\rho}}{D^2 (\Delta p)^{3/2}}$ (1)

Turbine pressure coefficient: $\psi_{tp} = \frac{\omega D \sqrt{\rho}}{\sqrt{\Delta p}}$ (2)

Turbine damping coefficient: $\psi_{td} = \frac{Q\sqrt{\rho}}{D^2\sqrt{\Delta p}}$ (3)

Here W_{out} is the instantaneous power output values obtained.

The change in the power coefficient values with the variation of pressure coefficient was obtained for cases of different cycle time as shown in Fig. 10. It can be seen that the ψ_{tw} values increase with the increase of ψ_{tp} values. The maximum value of ψ_{tw} is 0.04 which is obtained for the 6s TP at the ψ_{tp} value of 0.47. The maximum ψ_{tw} value keeps decreasing with increasing cycle time and has a minimum value of 0.013 for the ψ_{tp} value of 0.175 for 12sec TP.

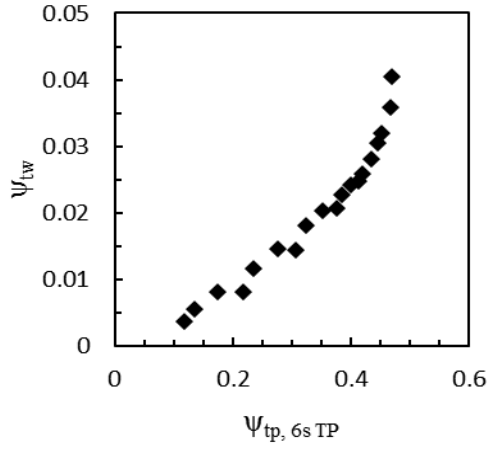

(a)

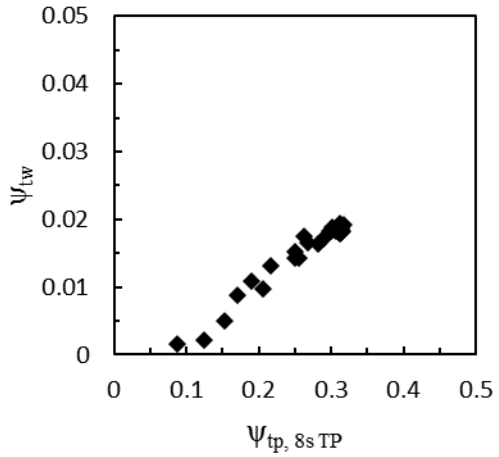

(b)

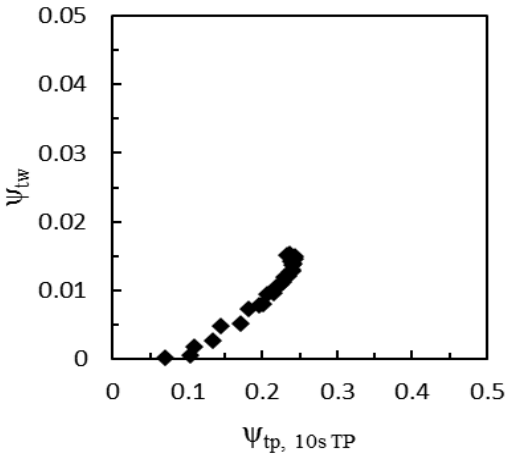

(c)

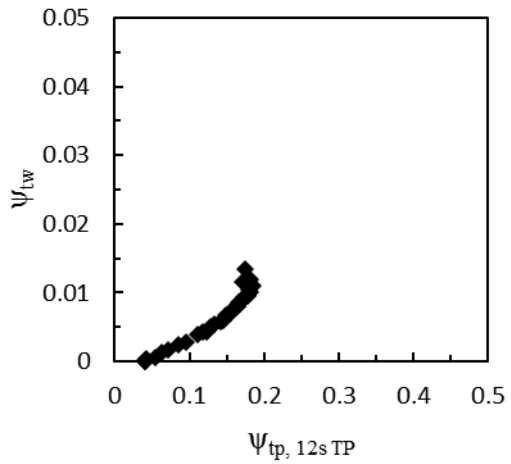

(d)

Fig. 10. Turbine power coefficient with respect to turbine pressure coefficient for different time periods

The Fig. 11 shows ψ_{td} variations with the change in ψ_{tp}.It is seen that the peak damping values are dominated by the acceleration part of the half cycle. As seen from the previous discussion the maximum ψ_{tw} for each TP corresponds to the maximum ψ_{tp} achieved during that cycle. Thus it can also be concluded that the value of ψ_{td}

corresponding to the maximum value of ψ_{tp} needs to be achieved for getting maximum ψ_{tw}.The information of optimum damping can also be used to determine the dimension of a suitable OWC for it [16].

VI. CONCLUSION

The following conclusion was made after analyzing the data of the experiment conducted.

- The pressure drop achieved across the turbine depends on the flow rate in the duct. The pressure variations are also slightly different during the cycle inhale and exhale, which is due to the losses occurring because of generator mounting.

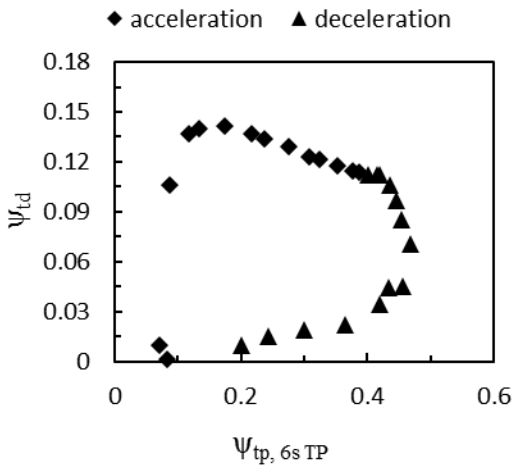

(a)

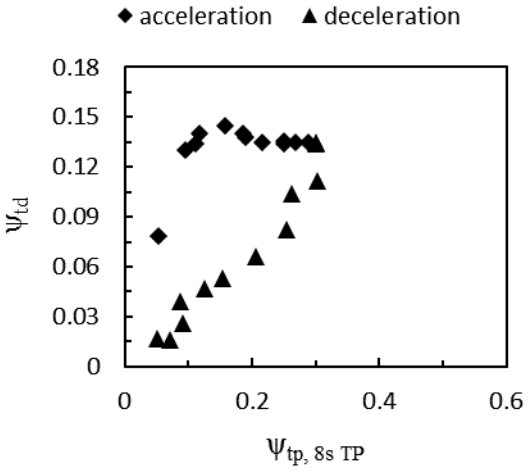

(b)

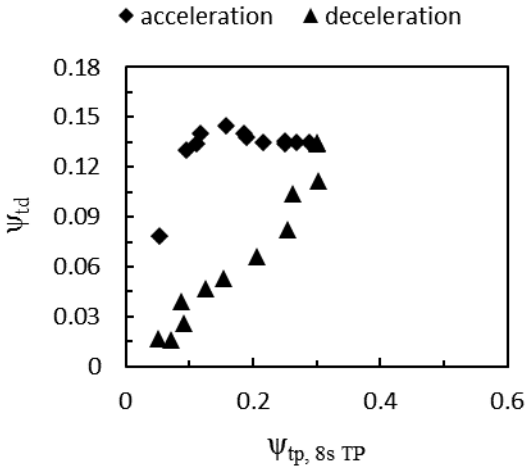

(c)

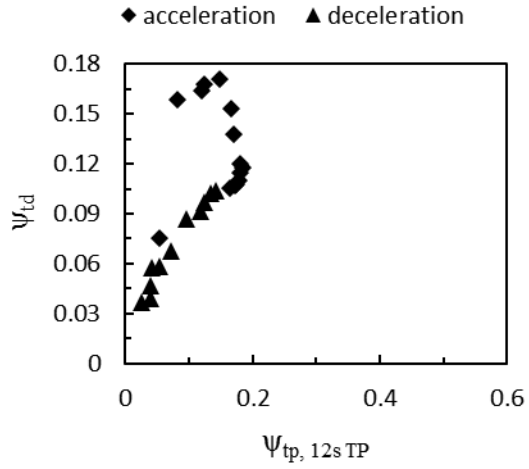

(d)

Fig. 11. Turbine damping coefficient with respect to turbine pressure coefficient for different time periods.

- The RPM of the turbine rotor depends on the flow rate of air. For larger flow rate, greater RPM was achieved.
- The turbine power coefficient increases or decreases with the increase or decrease of the turbine pressure coefficient. Also for lower time periods (keeping the stroke length constant), the value of the turbine power coefficient is more. Maximum turbine power coefficient value for each case is seen at the point of maximum turbine pressure coefficient value.
- For every cycle, there is a certain turbine damping coefficient value which is optimum, corresponding to the maximum turbine pressure coefficient value. Thus the maximum power

coefficient value can be achieved if we maintain the obtained optimum damping coefficient value.

NOMENCLATURE

Acronyms

BDI	Bi-directional impulse turbine
DGV	Downstream guide vane
GV	Guide vane
H/T	Hub to tip ratio
OWC	Oscillating water column
SLS	Selective laser sintering
TP	Time period
TP_{max}	Maximum time period
UDI	Uni-directional impulse turbine
UGV	Upstream guide vane
VFD	Variable frequency drive

Symbols

Δp	Pressure drop
Δp^*	Non-dimensional pressure drop
Δp_{max}	Maximum pressure drop
D	Turbine tip diameter
Q	Flow rate
Q^*	Non-dimensional flow rate
Q_{max}	Maximum flow rate
t	time
W_{out}	Instantaneous power output obtained
ρ	Fluid density
Ψ_{td}	Turbine damping coefficient
Ψ_{tp}	Turbine pressure coefficient
ω	Angular speed

REFERENCES

[1] B. Drew, A. R. Plummer and M. N. Sahinkaya, "A review of wave energy converter technology," *Proceedings of the Institution of Mechanical Engineers, Part A: Journal of Power and Energy*, vol. 223, pp. 887–902, 2009.

[2] J. Falnes, "A review of wave-energy extraction," *Marine Structures*, vol. 20, pp.185-201, 2007

[3] A. F. O. Falcão and J. C. C. Henriques, " Oscillating-water-column wave energy converters and air turbines: A review," *Renewable Energy*, vol. 85, pp. 1391-1424, 2016.

[4] T. V. Heath, "A review of oscillating water columns," *Philos. Trans. R. Soc. A Math. Phys. Eng. Sci.*, vol. 370, no. 1959, pp. 235–245, 2012.

[5] H. Maeda, S. Santhakumar, T. Setoguchi, M. Takao, and K. Kaneko, "Performance of an impulse turbine with fixed guide vanes for wave power conversion," *Renewable energy*, vol.17, pp. 533-547

[6] M. Inioue, K. Kaneko and T. Setoguchi, "One-dimensional analysis of impulse turbine with self-pitch-controlled guide vanes for wave power conversion, "*International Journal Of Rotating Machinery*, vol. 6, no. 2, pp. 151–157, 2000.

[7] A. Thakker, P.Frawley and H. B. Khaleeq, "An investigation of the effects of reynolds number on the performance of 0.6m impulse turbines for different hub to tip ratio," *Proceedings of the Twelfth International Offshore and Polar Engineering Conference*, Kitakyushu, Japan2002

[8] A. Thakker, Z. Usmani and T. S. Dhanasekaran, "Effects of turbine damping on performance of an impulse turbine for wave energy conversion under different sea conditions using numerical simulation techniques," *Renewable Energy*, vol. 29, no. 14, pp. 2133–2151, 2004.

[9] S. Santhakumar, V. Jayashankar, M.A. Atmallmul, A. G. Pathak, M. Ravindran, T. Setoguchi, M. Takao, and K. Kaneko, "Performance of an impulse turbine based wave energy plant," *Eighth International Offshore And Polar Engineering Conference, Montreal, Canada*, vol. 1, 1998.

[10] I. Lopez, B. Pereiras, F. Castro, and G. Iglesias, "Holistic performance analysis and turbine-induced damping for an OWC wave energy converter," *Renewable Energy*, vol. 85, 2016.

[11] I. Lopez, G. Iglesias, "Efficiency of OWC wave energy converters : A virtual laboratory,"*Applied Ocean Research*, vol. 44, pp. 63–70, 2014.

[12] A. George, B. Ranjith, P.V. Dudhgaonkar, A. Samad, "Evaluation of impulse turbines for a wave energy converter," *ASME Gas Turbine India Conference*, Bangalore, India, 2017

[13] A. George, R. Anandanarayanan, R. Suchithra, P. Dudhgaonkar, P. Jalihal, A. Samad and B. Pattnaik "Experimental analysis of turbine-chamber coupling for wave energy conversion,", *International Journal*

Of Energy Research, vol. 40, pp. 7770–7782, 2018.

[14] R. Badhurshah, A. Samad, "Multiple surrogate-based optimization of a bidirectional impulse turbine for wave energy conversion," *Renewable Energy*, vol. 74, pp. 749-760, 2015.

[15] T. Ghisu, P. Puddu, F. Cambuli, "Physical explanation of the hysteresis in wells turbines: a critical reconsideration," *Journal of Fluids Engineering*, vol 138, 111105-1, 2016.

[16] B. Pereiras, I. Lopez, F Castro, G. Iglesias, "Non-dimensional analysis for matching an impulse turbine to an OWC (oscillating water column) with an optimum energy transfer, " *Energy*, vol. 87, 481-489, 2015.